the nominal (macroscopic) elongation α of the specimen, however.

Making comparisons at $\alpha = 2$, we note from the work of Read and Stein[1] that $D - 1 \approx 4.5$ for the 2016-cm^{-1} combination band representing *trans* sequences ... *tttt*... of more than four bonds. The transition moment is parallel to the a' axis (Figure 1C). Our calculations, with $\sigma = 0.544$ and $\omega = 0.0875$, give $G_2^*(a') = 6.7$ for the *tttt* conformation. The values of $D - 1$ and G_2^*(calculated) are not to be compared directly; they are significant only in relation to values for other bands.

For the 1352-cm^{-1} wagging frequency of the CH$_2$ group situated between *gauche* ($g^{\pm}g^{\pm}$) bonds, Read and Stein found $D - 1 \approx 0.3$ at $\alpha = 2$. Its transition moment is in the direction of axis a' (Figure 1C). Our calculations yield $G_2^*(a') = 1.1$.

The transition moment for the 1303-cm^{-1} band, representing wagging of the CH$_2$ groups in $g^{\pm}tg^{\pm}$ and $g^{\pm}tg^{\pm}$ conformations, is directed between the a and b axes of Figure 1A. According to Read and Stein, $D - 1 \approx 0.1$ at $\alpha = 2$. Our calculations, confined to symmetry axes taken individually, yield $G_2^*(a) = -1.4$ and -2.4 for the $g^{\pm}tg^{\mp}$ and $g^{\pm}tg^{\mp}$ conformations, respectively, and $G_2^*(b) = 3.7$ and 2.7 correspondingly for the b axis. Hence, the calculated results are consistent with a value of $D - 1$ near zero.

The 1078-cm^{-1} band is attributed[1,11] to C—C bond stretching for both t and g conformations. The transition dipole for the former is very small owing to the centrosymmetry of the bond in this conformation. Hence, this band may be assumed to arise preponderantly from *gauche* bonds. The transition moment is parallel to c' (Figure 1B). According to the results of Read and Stein,[1] $D - 1 = -0.3$ at $\alpha = 2$. We obtain $G_2^*(c') = -2.1$.

Qualitative agreement between the calculated preferential orientations and infrared dichroic measurements is demonstrated by these comparisons. It is noteworthy that the conventional model of a chain comprising freely jointed segments is incapable of interrelating dichroism and the location of the transition moment within the skeletal structure of the real chain.

Acknowledgment. This work was supported by the Directorate of Chemical Sciences, U. S. Air Force office of Scientific Research Contract No. F 44620-69-C-0058.

(11) R. G. Snyder, *J. Chem. Phys.*, **47**, 1316 (1967).

On the Statistical Thermodynamics of Spherical and Chain Molecule Fluids

Robert Simha[1a] **and Thomas Somcynsky**[1b]

Department of Chemistry, University of Southern California,
Los Angeles, California 90007. *Received March 12, 1969*

ABSTRACT: An improvement of the cell model for the liquid state by the introduction of vacancies in the lattice is considered. Two alternative assumptions (I and II), relating the cell partition function to the equilibrium fraction of vacancies, are employed. In I we average linearly over "solidlike" and "gaslike" free lengths or modes of motion, and in II over the free volumes themselves. The square-well approximation to the cell potential is used and nonnearest neighbor contributions to the lattice energy are included. The theory is applied to both spherical and chain molecules. In the liquid state, the properties studied are the equation of state, the cohesive energy, the internal entropy, and the internal pressure. For spherical molecules, critical and vapor pressure data and isotherms in the dense gas region are also computed. The comparison with experimental data of argon makes use of the reducing factors derived from second virial coefficients. Formulation I is found to be considerably superior to both the cell model and assumption II. For polymers a superposition procedure must be used for purposes of comparison. In contrast to the cell theory, the hole theory, in either formulation, describes accurately the experimental reduced zero pressure isobar over the whole range. Although promising, no decisive superiority over the cell theory in respect to other properties is observed in the present formulation. The theory does not lead strictly to a principle of corresponding states, but the resulting families of curves are practically superimposable. In order to compare the relative position of theory and experiment for the two types of liquids, the analysis of argon data is repeated by means of a superposition procedure. Differences appear in respect to the internal pressure and the compressibility, suggesting that the basic steps used to make the transition from spherical to chain fluids must be reexamined.

I. Introduction

In recent years increasing attention has been given to finding general relations which describe thermodynamic properties of chain molecule liquids and amorphous polymers. In addition to the intrinsic problem in the theory of the liquid state, these relations are needed in order to estimate physical properties under conditions unavailable experimentally and as a tool in the study of mixtures. The transition from the theoretical approach for spherical molecules to the case of chain liquids was made possible by Prigogine's introduction[2a] of the concept of external degrees of freedom. Subsequently,

---

(1) (a) Division of Macromolecular Science, Case Western Reserve University, Cleveland, Ohio 41106. (b) Département de Chimie, Université de Sherbrooke, Sherbrooke, P. Q., Canada.

(2) (a) I. Prigogine, "The Molecular Theory of Solutions," North Holland Publishing Co., Amsterdam, 1957; (b) J. Hijmans, *Physica*, **27**, 433 (1961).

Hijmans[2b] formulated necessary conditions for the existence of a phenomenological principle of corresponding states.

In previous work[3–5] the equation of state and related properties of several oligomer and polymer systems were shown to conform to corresponding state relations. The master curve describing the behavior of these substances was compared with the predictions of the cell model, in particular using the square-well approximation. It was found that the agreement between theory and experiment is limited to the zero pressure isobar[3] and the cohesive energy density[5] in a range of reduced volumes $\tilde{V}$ between 1.0 and 1.2. The model fails in describing the internal pressure and the compressibility.

It is well known that the cell model ascribes to the liquid a structure more appropriate to the solid state and hence does not yield enough entropy. By allowing for empty sites, a mixing term is added to the entropy, which may correct this deficiency of the cell theory, while retaining much of the tractability of the model. The critical step here is the nature of the assumption regarding the dependence of the free volume on the number of empty sites. Two general expressions have been proposed for spherical molecules. One is based[6] on a linear dependence of the logarithm of the free volume on the number of vacancies and the other on a linear dependence of the free volume itself. The various theories proposed differ in the choice of the combinatory factor and in some details of the linear relations just mentioned.

We have already presented the general formalism for the introduction of holes in a lattice occupied by chain molecules.[5] The consequences of the linerization of the logarithm of the free volume and the complications arising from the chain character of the molecule were discussed at that occasion. For argon, on the other hand, the best agreement has been observed with a free volume which varies linearly with the number of vacancies.[7–9] As in the method of significant structures[10] this relation is based on the idea that a spherical molecule acquires gaslike properties when neighboring a hole. However, in the cell model employed for chain liquids, the free volume contribution of a molecule is factorized[1] into $3c$ elements, where $3c$ is the number of independent external degrees of freedom. Thus averaging over individual modes of motion or degrees of freedom may represent a physically more satisfactory assumption than averaging over units of three degrees of freedom. We shall test the assumption that only the motion in the direction of a neighboring vacancy is affected for spherical molecules as well.

For rare gas fluids, the method of molecular distribution functions has been extensively explored in recent years by means of various alternative approximations and has resulted in some notable numerical successes.[11] Also Weissmann[12] has explored by means of Monte Carlo computations the actual dependence of the free volume on the fraction of vacancies. The isotherm calculated near the critical temperature disagrees with experiment for argon. However, this does not necessarily indicate an inadequacy of the free volume model. The size of the sample used and the requirement for accurate derivatives of the computed function may be the cause of the discrepancy. In this connection one of us[13] has shown that eq 1 in section II, with a free volume function derived from experiment and consistent with a minimization of the free energy, predicts several additional properties of argon very well. Finally, the free volume approach, in contrast to the molecular distributions function theories, at least by analytical procedures, permits a ready generalization for chain liquids.

In this paper we explore the applicability of the two alternative linearizations of the external degrees of freedom mentioned above. Our primary interest is the amorphous polymer. However, it becomes desirable and actually necessary for two reasons to investigate monomer-type systems as well. For several simple liquids, the reducing parameters are known and no disposable constants remain. For polymers, on the other hand, the comparison with a theory expressed in dimensionless variables requires by necessity a superposition procedure, since we have no independent knowledge of the reducing parameters. Second, by comparing in the same manner the position of the theory *vis à vis* experiment for the two types of systems, the consequences of introducing the additional parameter c should become apparent. We shall use argon where detailed experimental data are available. Moreover it has served previously as a test substance for comparisons with theory and it is representative for a whole class of substances which satisfy an experimental principle of corresponding states. The theoretical development is presented in the next section. It will be convenient to evaluate the simpler case of argon (section III) before dealing with the polymer liquid (section IV).

II. Theoretical Development

We write the configurational partition function for a system of N s-mer molecules, occupying a fraction y of the total number of available sites, as

$$Z = g(N, y)[v_f(V, y)]^{cN} \exp[-E_0(V, y)/kT] \qquad (1)$$

where g represents the combinatory factor, arising from the mixing of molecules and unoccupied sites, v_f the free volume per each three of the total number $3c$ of external degrees of freedom attributed to a chain, and E_0 the potential energy of the system with all segments placed in their rest positions. We shall assume the holes to be of uniform size and obtain the factor g from the theory of Flory and of Huggins. Retaining the part pertinent for our purposes, one has[5]

$$g(N, y) \propto y^{-N}(1 - y)^{-Ns(1-y)/y} \qquad (2)$$

---

(3) V. S. Nanda and R. Simha, *J. Phys. Chem.*, **68**, 3158 (1964).

(4) V. S. Nanda and R. Simha, *J. Chem. Phys.*, **41**, 3870 (1964).

(5) V. S. Nanda, R. Simha, and T. Somcynsky, *J. Polym. Sci., Part C*, **12**, 277 (1966).

(6) J. S. Rowlinson and C. F. Curtiss, *J. Chem. Phys.*, **19**, 1519 (1951).

(7) D. Henderson, *ibid.*, **37**, 631 (1962).

(8) A. G. McLellan, *ibid.*, **40**, 567 (1964).

(9) G. E. Blomgren, *ibid.*, **38**, 1714 (1963).

(10) H. Eyring, D. Henderson, B. J. Jones, and E. W. Eyring, "Statistical Mechanics and Dynamics," John Wiley & Sons, New York, N. Y., 1964.

(11) See, for example, J. A. Barker and D. Henderson, *J. Chem. Phys.*, **47**, 4714 (1967).

(12) M. Weissmann, *ibid.*, **40**, 175 (1964).

(13) T. Somcynsky, unpublished.

and for E_0, introducing the cell volume $\omega = yV/(Ns) = yv$

$$2E_0 = yNqz\epsilon^*[1.011(v^*/\omega)^4 - 2.409(v^*/\omega)^2] \quad (3)$$

The quantities ϵ^* and v^* represent, as usual, the characteristic energy and volume per segment and qz the number of nearest neighbor sites per chain, equal to $s(z - 2) + 2$, z being the coordination number. In terms of these quantities the reduced variables of state are

$$\tilde{V} = V/(Nsv^*) = v/v^*$$
$$\tilde{T} = ckT/(qz\epsilon^*)$$
$$\tilde{p} = psv^*/(qz\epsilon^*) \quad (4)$$

Thus a geometric (s) and a dynamic (c) parameter describe the chain character of a molecule. As discussed in the Introduction, we write for the free volume the following alternative expressions as functions of y and the reduced cell volume $\tilde{\omega}$

$$\tilde{v}_f = v_f/v^* = [y(\tilde{\omega}^{1/3} - 2^{-1/6}) + (1 - y)\tilde{\omega}^{1/3}]^3 \quad \text{(I-5)}$$

$$\tilde{v}_f = y(\tilde{\omega}^{1/3} - 2^{-1/6})^3 + (1 - y)\tilde{\omega} \quad \text{(II-5)}$$

where each first term represents a "solidlike" and each second one a "gaslike" contribution.[7] In assumption I we average linearly over single modes of motion, and in II over free volumes, *i.e.*, over units of three degrees of freedom. Equation II-5 is basically identical with Henderson's expression. The difference lies in the simplifying replacement of the Lennard-Jones and Devonshire free volume for the solidlike part by the square-well approximation. Actually, the specific nature of this term is not important here, since the gaslike contribution strongly predominates in the final result. In eq I-5 on the other hand, it will turn out that both components contribute significantly in the pertinent range of variables, the first part being more important at sufficiently low temperatures, as it should. We have nevertheless retained the square-well approximation throughout. There will appear, however, significant differences for spherical fluids between Henderson's and our numerical results in assumption II. These arise essentially from the choice of the potential E_0. In eq 3 the contribution of nonnearest neighbor shells is included whereas Henderson retains only the first shell interactions. The numerical coefficients in eq 3 would therefore be 1 and 2, respectively.

To obtain the free energy as a function of V and T we require the function $y(V, T)$. It will be obtained by the minimization of the Helmholtz free energy or

$$(\partial Z/\partial y)_{V,T} = 0 \quad (6)$$

From eq 1–5 we find

$$(s/3c)[(s - 1)/s + y^{-1}\ln(1 - y)] = L(y, \tilde{V}) + (y/6\tilde{T})(y\tilde{V})^{-2}[2.409 - 3.033(y\tilde{V})^{-2}] \quad \text{(I, II-6)}$$

with

$$L_{\text{I}} = [2^{-1/6}y(y\tilde{V})^{-1/3} - {}^1/_3][1 - 2^{-1/6}y(y\tilde{V})^{-1/3}]^{-1}$$

$$L_{\text{II}} = ({}^1/_3)\{2y - 1 - y[1 - 2^{-1/6}(y\tilde{V})^{-1/3}]^2 - y[1 - 2^{-1/6}(y\tilde{V})^{-1/3}]^3\}\{1 - y + y[1 - 2^{-1/6}(y\tilde{V})^{-1/3}]^3\}^{-1}$$

Equations 1–6 apply to both chain liquids and spherical fluids. For the latter the expressions are obtained by setting $s = c = q = 1$.

From the relations $p = -(\partial F/\partial V)_T$ and $V(\partial F/\partial\omega)_{V,T} = (\partial F/\partial y)_{V,T}$, one derives

$$p = -(\partial F/\partial V)_{T,\omega} = (y/V)(\partial F/\partial y)_{T,\omega}$$

and the reduced equation of state

$$\tilde{p}\tilde{V}/\tilde{T} = M(y, \tilde{V}) + (2y/\tilde{T})\cdot (y\tilde{V})^{-2}[1.011(y\tilde{V})^{-2} - 1.2045] \quad \text{(I, II-7)}$$

with

$$M_{\text{I}} = [1 - 2^{-1/6}y(y\tilde{V})^{-1/3}]^{-1}$$

$$M_{\text{II}} = \{1 - y + y[1 - 2^{-1/6}(y\tilde{V})^{-1/3}]^2\} \times \{1 - y + y[1 - 2^{-1/6}(y\tilde{V})^{-1/3}]^3\}^{-1}$$

We observe that y in eq (I, II-6) is a function of the chain length s and the ratio s/c and does not depend on the reduced variables, eq 4, solely. Hence, formally, this theory does not lead to a principle of corresponding states for chain fluids, even when the well-known conditions on the potential are met. A consideration of this point will be postponed until section IV.

Next we obtain the expression for the reduced cohesive energy density (cẽd) $-\tilde{U}/\tilde{V}$, *viz.*

$$-\tilde{U}/\tilde{V} = (y/2\tilde{V})(y\tilde{V})^{-2}[2.409 - 1.011(y\tilde{V})^{-2}] \quad (8)$$

and the reduced internal pressure, $(\partial\tilde{U}/\partial\tilde{V})_{\tilde{T}}$, *viz.*

$$\tilde{p}_i = ({}^1/_2)(y\tilde{V})^{-2}[2.409 - 3.033(y\tilde{V})^{-2}](\partial y/\partial\tilde{V}) + (2y/\tilde{V})(y\tilde{V})^{-2}[1.2045 - 1.011(y\tilde{V})^{-2}] \quad (9)$$

The difference between the two assumptions (eq 5) resides in the actual magnitudes of the y values and their derivatives. For the latter we have

$$(\tilde{V}/y)(\partial y/\partial\tilde{V})_{\tilde{T}} = \{Q - (y/2\tilde{T})(y\tilde{V})^{-2}[12.132(y\tilde{V})^{-2} - 4.818]\}\{R + (y/2\tilde{T})(y\tilde{V})^{-2}[9.099(y\tilde{V})^{-2} - 2.409] + (s/c)[y^{-1}\ln(1 - y) + 1/(1 - y)]\}^{-1} \quad \text{(I, II-10)}$$

where

$$R_{\text{I}} = 2Q_{\text{I}} = ({}^4/_3)M_1M_{\text{I}} - 1)$$

$$Q_{\text{II}} = (1 - X)[X^3 + (1 - y)/y]^{-1} \times [X^2(1 + 3\text{L}_{\text{II}}) + 2X/3]$$

$$R_{\text{II}} = (1/y)[X^3 + (1 - y)/y]^{-1}(1 + 3\text{L}_{\text{II}}) - \text{Q}_{\text{II}}$$

and

$$X = 1 - 2^{-1/6}(y\tilde{V})^{-1/3}$$

By setting $y = 1$ in all the preceding equations, we recover the corresponding expressions for the cell model in the square-well approximation.

III. Spherical Molecule Fluids

We will compare the preceding theoretical expressions, specialized to $s = c = q = 1$, with experimental data for argon, after reduction by means of the pair potential constants[14] $\epsilon^*/k = 119.8$°K and $\sigma = 3.405$ Å. In order to facilitate the comparison with other theories, we conform in this section to the definitions generally used for spherical fluids, *i.e.*, $\tilde{T} = kT/\epsilon^*$, cẽd = ced($v^*/\epsilon^*$), etc., in which the constant z is omitted in the reducing factor for the energy and hence appears explic-

(14) J. M. H. Levelt, *Physica*, **26**, 361 (1960).

TABLE I
COMPUTED REDUCED THERMODYNAMIC PROPERTIES AT ZERO PRESSURE FOR SPHERICAL FLUIDS

$\tilde{V}$	$\tilde{\omega}$	$\tilde{T}$	$\widetilde{\text{céd}}$	$\tilde{p}_i$
		Assumption I		
1.0	0.9601	0.3579	8.200	5.556
1.1	0.9633	0.5468	6.972	5.434
1.2	0.9661	0.6888	5.718	4.900
1.3	0.9688	0.7979	4.881	4.345
1.4	0.9714	0.8824	4.215	3.845
1.5	0.9739	0.9482	3.678	3.411
1.6	0.9764	0.9996	3.237	3.039
		Assumption II		
1.0	0.9247	0.5314	7.959	3.673
1.1	0.9325	0.9394	6.627	4.484
1.2	0.9393	1.2135	5.603	4.364
1.3	0.9454	1.4035	4.799	4.018
1.4	0.9510	1.5365	4.156	3.634
1.5	0.9562	1.6294	3.635	3.270
1.6	0.9610	1.6933	3.205	2.942

itly in the thermodynamic expressions. We adopt the value $z = 12$ and the computed values of $\tilde{T}$, cẽd and $\tilde{p}_i$ presented here are then twelve times those obtained with the general expressions derived in the preceding section.

In Table I are presented some results for low pressures. The procedure to be followed is to set $\tilde{p} = 0$ in eq 7 and to obtain an expression for $\tilde{T}$ as a function of y and $\tilde{V}$. Values of y as a function of V at zero pressure then follow from eq 6, after introducing the expression for $\tilde{T}(y, \tilde{V})$. Once the values of y are known, all other properties are readily derived. The striking fact in Table I is the approximate constancy of the cell size, especially with assumption I. This means that nearly the whole expansion of the liquid is attributed by the theory to a continuous introduction of vacancies, as shown by a sharp decrease of the fraction $y = \tilde{\omega}/\tilde{V}$ with increasing temperature. At this point we recall the X-ray scattering results for argon by Eisenstein and Gingrich[15] and the neutron diffraction data on krypton by Clayton and Heaton.[16] In both instances the whole liquid range up to the critical point was covered. In both liquids, the increase of the nearest neighbor distance with temperature is minimal, whereas the number of nearest neighbors decreases markedly. The qualitative picture emerging from these experiments is then very similar to that deduced from the hole theory, provided a dependence of the free volume on the number of empty sites of type eq I-5 or II-5 is assumed. It has been noted earlier[7] that when the logarithm of the free volume is linearized, the minimization of the free energy is generally brought about by an increase of the cell size, rather than by the introduction of holes, leading to results not too different from those of the cell theory. It is interesting to note that a strictly constant cell size together with eq 8 leads to the van der Waals form for the cohesive energy, in contrast to the result of cell theories, but in accord with empirical expressions.

Several physical properties are examined next. Figure 1 shows the $\tilde{V}$–$\tilde{T}$ relation at zero pressure for argon, assumptions I and II and other statistical mechanical models.[17] The predictions of assumption I are much better than those of II and compare well with the other theories displayed in this figure, although they are not as good as the results of the tunnel model.

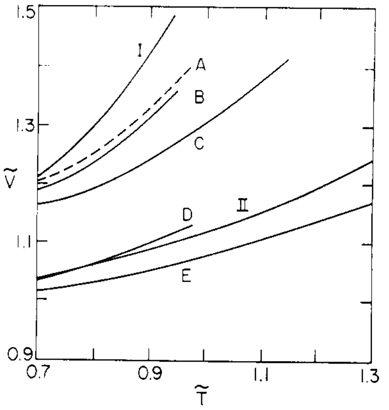

Figure 1. Reduced volume–temperature relation at low pressure for liquid argon: A, experimental; I and II, eq I, II-7; B, C, D, E, respectively, tunnel, worm, Lennard-Jones and Devonshire, Dahler, and Hirschfelder, according to ref 17.

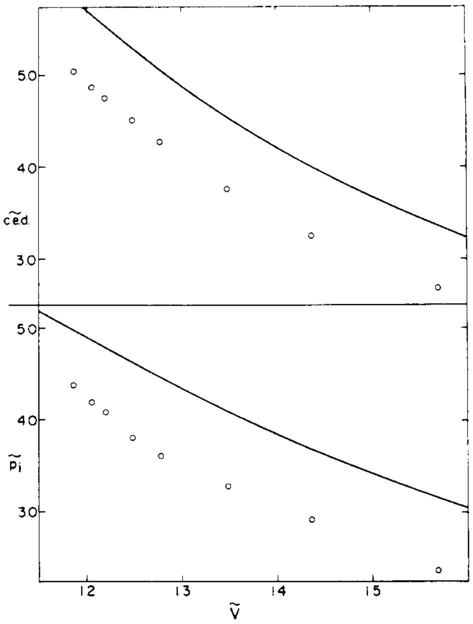

Figure 2. Reduced cohesive energy density and internal pressure as a function of reduced volume for liquid argon: curves, eq 8 and 9 with assumption I, points, experimental.

In Figure 2 we compare assumption I with the cohesive energy density and the internal pressure of argon in the liquid range, taken from the data tabulated by Rowlinson,[18] with the volume as the independent variable. The agreement can be considered quite satisfactory. From Table I it is seen for $\tilde{V} > 1.2$ that the results obtained with assumption II are similar if the volume is used as the independent variable, but very different with temperature as the independent variable.[19]

---

[15] A. Eisenstein and N. S. Gingrich, *Phys. Rev.*, **62**, 261 (1942).

[16] G. T. Clayton and LeRoy Heaton, *ibid.*, **121**, 649 (1961).

[17] This figure is reproduced from a paper of H. S. Chung and J. S. Dahler, *J. Chem. Phys.*, **43**, 2606 (1965), to which we have added curves I and II.

[18] J. S. Rowlinson, "Liquids and Liquid Mixtures," Butterworth and Co., Ltd., London, 1959.

[19] D. Henderson, *J. Chem. Phys.*, **39**, 54 (1963).

Table II
Computed and Experimental Reduced Critical Constants

	Ref	$\tilde{V}_c$	$\tilde{T}_c$	$\tilde{p}_c$	$\tilde{p}_c\tilde{V}_c/\tilde{T}_c$
Expt (argon)	7	3.16	1.26	0.116	0.29
I		3.9	1.27	0.115	0.35
II		3.0	2.07	0.246	0.36
Henderson	7	3.39	1.42	0.139	0.33
Tunnel	17	1.8	1.07	0.37	0.60
Worm	17	2.8	1.5	0.44	0.82
Peek and Hill	7	3.25	1.18	0.261	0.72
Lennard-Jones and Devonshire	7	1.77	1.30	0.434	0.59

Table III
Computed Equilibrium Values of the Cell Size $\tilde{\omega}$, at Different Volumes and Temperatures

	$\tilde{T}$					
$1/\tilde{V}$	1.20	1.30	1.50	2.0	2.5	3.0
			Assumption I			
0.05	1.0219	1.0158	1.0040	0.9778	0.9552	0.9353
0.10	1.0184	1.0121	1.0001	0.9735	0.9506	0.9305
0.20	1.0106	1.0040	0.9916	0.9640	0.9405	0.9200
0.30	1.0016	0.9947	0.9817	0.9533	0.9292	0.9084
0.40	0.9910	0.9838	0.9704	0.9411	0.9165	0.8954
0.50	0.9785	0.9710	0.9571	0.9270	0.9021	0.8808
0.60	0.9635	0.9557	0.9414	0.9108	0.8856	0.8643
0.70	0.9453	0.9374	0.9228	0.8919	0.8667	0.8455
			Assumption II			
0.05	1.0498	1.0450	1.0358	1.0150	0.9966	0.9802
0.10	1.0468	1.0419	1.0325	1.0112	0.9925	0.9757
0.20	1.0400	1.0348	1.0249	1.0027	0.9832	0.9660
0.30	1.0319	1.0264	1.0160	0.9927	0.9726	0.9550
0.40	1.0221	1.0162	1.0053	0.9810	0.9603	0.9423
0.50	1.0099	1.0038	0.9922	0.9671	0.9460	0.9277
0.60	0.9946	0.9882	0.9762	0.9505	0.9291	0.9108
0.70	0.9751	0.9685	0.9563	0.9305	0.9092	0.8912

Figure 2 together with eq 8 indicates that the computed fraction of vacancies is smaller than that required to fit the experimental ced.

Next we consider the critical data and the vapor–liquid equilibrium. The former are obtained by an examination of a series of $\tilde{p}$–$\tilde{V}$ curves in the critical region. Several theoretical results are compared in Table II with experimental values for argon. It is seen that our predictions for the critical temperature and pressure are very good indeed with assumption I, but less so for the critical volume. The computed critical compressibility factor is quite satisfactory. By comparison, the predictions of assumption II are rather poor, especially for the temperature. Figure 3 depicts the "rectilinear diameters" plot[20] for assumption I. It was derived by searching analytically for common tangents to the $\tilde{F}$–$\tilde{V}$ function in the liquid and vapor region at each temperature. The reduced theoretical and experimental[6] relations for the vapor pressure are, respectively

$$\log \tilde{p} = 1.53 - 3.14/\tilde{T} \qquad \text{(I-11)}$$

$$\log \tilde{p} = 1.29 - 2.84/\tilde{T} \qquad (12)$$

The agreement is good, and increasingly so on approaching the critical region. From eq I-11 we obtain for p = 1 atm, T_b = 90.7°K, compared with the experimental value of 87.29°K.

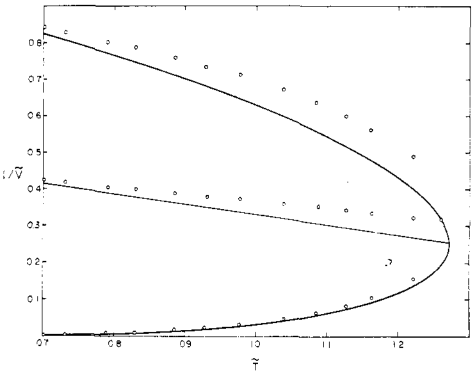

Figure 3. Reduced rectilinear diameters plot for argon: curve, theory, assumption I; points, experimental.

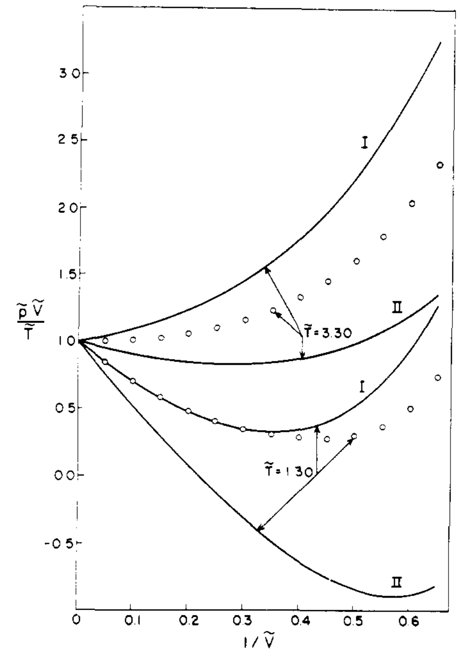

Figure 4. Reduced compressibility factor as a function of reduced density for gaseous argon at two reduced temperatures: curves, theory, eq I, II-7; points, experimental.

The compressibility factor was computed with eq I-7 and II-7 for the experimental range covered by the tabulation of Levelt.[14] The pertinent equilibrium cell sizes are listed in Table III. In Figure 4 we present two typical results, near the critical region and at a higher temperature. The experimental data are located in general between the predictions of assumptions I and II. When the free volume is computed by averaging over modes of motion the compressibility is too small, whereas by averaging the solid and gaslike free volumes one obtains too large a compressibility. Figure 5 shows the internal entropy in the liquid range, *i.e.*, the negative excess relative to the perfect gas at the same V and T. Again the observed values lie between I and II. The former, yielding too small a compressibility, also predicts too low an entropy. The model used should be rather crude for the dense gas, but the vacancies pro-

---

(20) The experimental values are taken from F. Din, "Thermodynamic Functions of Gases," Vol. 2, Butterworth and Co., Ltd., London, 1962.

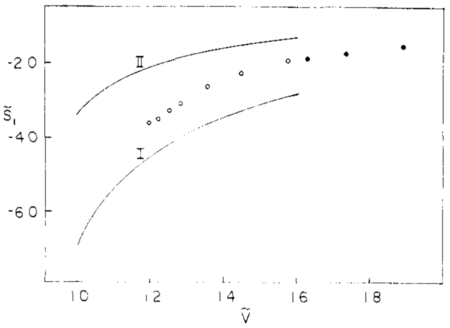

Figure 5. Reduced internal entropy (S_I/Nk) as a function of reduced volume for liquid argon: curves assumptions I and II; points—●, from A. Michels, J. M. Levelt, and G. J. Wolkers, *Physica*, **24**, 769(1958); ○, computed from data in the following sources [P. J. Hunter and J. S. Rowlinson, "Simple Dense Fluids," H. L. Frisch and Z. W. Salsburg, Ed., Academic Press, New York, N.Y., 1968, p 1; G. A. Cook, "Argon, Helium and the Rare Gases," Vol. I. Interscience Publishers, New York, N. Y., 1961; B. E. F. Fender and G. D. Halsey, *J. Chem. Phys.*, **36**, 1881(1962)].

vide nevertheless a notable improvement for these properties also.

In respect to several properties the results of assumption II differ considerably from those of Henderson.[7] We recall that this difference is essentially due to the choice of the constants appearing in the lattice energy, Hirschfelder, Curtiss, and Byrd[21] have indicated the pronounced influence of the higher order shells on the compressibility factors, based on the Lennard-Jones and Devonshire theory. The inclusion of higher order interactions represents a refinement of the model and the fact that a better agreement is obtained when they are omitted suggests some cancellation of errors. Basically, of course, some analogous reason may be the source of the agreement obtained with assumption I.

Guggenheim[22] has examined an equation of state resulting from the combination of the scaled particle theory for hard spheres with a van der Waals cohesive term, as adopted originally by Longuet-Higgins and Widom.[23] Some of his results for argon at the triple point are shown in Table IV. Here temperature is the independent variable.

TABLE IV
COMPUTED AND EXPERIMENTAL QUANTITIES FOR ARGON AT THE TRIPLE POINT

	Exptl	Guggenheim	I	II
$(T/V)(\partial V/\partial T)_p$	0.37	0.57	0.47	0.16
$(V/R)(\partial p/\partial T)_v$	7.4	8.6	8.4	6.2
$\tilde{V}$	1.186	1.226[a]	1.209	1.036

[a] Assuming $\tilde{V} = \pi/(6y)$, with y defined in ref 23.

This completes the comparison between experiment and our theory. We have seen that with the assumed form of the potential, eq 3, and the square-well approximation, assumption I yields considerably better results than assumption II.

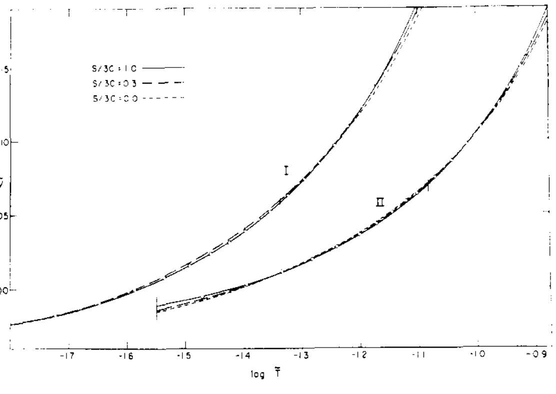

Figure 6. Reduced volume–temperature relation at atmospheric pressure for polymer liquids, various values of s/c and formulations I and II. The coordinate system corresponds to $s/3c = 1$.

IV. Chain Molecule Liquids

We now turn to the properties of polymers. The experimental information to be used is contained in the set of master curves obtained earlier.[3,5] At this point we recall that according to eq 6 y depends explicitly on s and s/c. A strict compliance with a principle of corresponding states would demand a functional dependence of y on s and c through reduced variables solely. It will turn out, however, as illustrated for instance in Figure 6, that the curves for different values of the ratio s/c are superimposable and hence a practical principle of corresponding states is derivable from our hole theory.

In order to obtain the characteristic reducing parameters from a superposition of experimental and theoretical curves, a previous knowledge of the values of s for oligomers, and s/c in all cases is required in order to construct the theoretical curves. It follows from what was said before that a unique numerical value of s/c for an infinite polymer can not be assigned from its equation of state. This is also true in the cell theory, but there the term s/c enters only into the definition of $\tilde{T}$ and is not required explicitly. To obtain self-consistent values for a given polymer series, an iteration procedure, involving oligomers, may be employed in conjunction with the analysis for finite molecular weights given earlier.[24] It was observed that the ratios $(s/n)/(s/n)_\infty$, $(c/n)/(c/n)_\infty$, and $(q/n)/(q/n)_\infty$ are linear in $1/n$, provided that ϵ^* and v^* are constant for the series and identical for terminal and middle segments. Moreover, these relationships are independent of the model used.[3] Selecting an arbitrary value of $(s/c)_\infty$, one obtains by superposition of V–T and ced–V data for the high polymer a set of numbers for $(s/n)_\infty$, $(c/n)_\infty$, ϵ^*, and v^*. These determine the corresponding first two quantities for a given finite n-mer by means of relations previously determined[24] or to be found from appropriate oligomer studies. On repeating the comparison between theory and experiment for the oligomer, values of ϵ^* and v^* are derived, which should be identical with the set obtained for the high polymer. If this is not the case, a second value of $(s/c)_\infty$ is chosen and the procedure repeated until constancy of ϵ^* and v^* is achieved. Of course, the

---

(21) J. O. Hirschfelder, C. F. Curtiss, and R. B. Byrd, "Molecular Theory of Gases and Liquids," John Wiley & Sons, New York, N. Y., 1954, p 299.

(22) E. A. Guggenheim, *Mol. Phys.*, **9**, 43 (1965).

(23) H. C. Longuet-Higgins and B. Widom, *ibid.*, **8**, 549 (1965).

(24) R. Simha and A. J. Havlik, *J. Amer. Chem. Soc.*, **86**, 197 (1964).

iteration can also be applied to a set of oligomers solely.

Computations of this type go beyond the purpose of this paper, which only explores to what extent a hole theory can describe the properties of chain liquids. Since the curves computed for widely different values of s/c are practically superimposable, only a few cases need to be considered. To solve the minimization condition we have assumed $s - 1 \simeq s$ and chosen for $s/3c$ the values 1.0, 0.3, and 0.0. The first corresponds to an idealized single bonded backbone with no barrier to internal rotation. This number will decrease if the chain becomes more flexible or if structured side groups are attached. The ratio $s/3c = 0.3$ represents a case where there are approximately three degrees of freedom per segment. Finally, as a lower limit, we have treated the case $s/3c \rightarrow 0$, although it does not represent a realistic system. The fact that the results obtained do not differ appreciably from each other indicates their insensitivity to variations in the quantity s/c and justifies the use of a single value in applying the equation of state. The superposition of experimental and theoretical master curves determines in each case a set of reducing factors and hence of *apparent* values for the constants ϵ^* and v^*. In Table V we indicate the values of the parameters relative to those derived from the cell theory.

Table V

Relation between Characteristic Parameters for Polymer Liquids in Cell Theory[a] and Hole Theory for Various Values of s/c

$s/3c$	$\tilde{V}/\tilde{V}_{\text{cell}}$	$\tilde{T}/\tilde{T}_{\text{cell}}$	$\tilde{p}/\tilde{p}_{\text{cell}}$
	Assumption I		
1.0	0.9506	0.4027	1.0563
0.3	0.9572	0.5012	1.0505
0.0	0.9616	0.5559	1.0448
	Assumption II		
1.0	0.9772	0.7211	0.9791
0.3	1.000	1.084	0.9424
0.0	1.014	1.365	0.9220

[a] See ref 3–5.

The predicted numbers of holes for spherical molecules and polymers turn out to be very similar. In Figure 6 a series of theoretical curves for assumptions I and II are shown, together with the experimental reduced $\tilde{V}$–$\tilde{T}$ function. In both instances the system of coordinates is defined by the choice $s/3c = 1.0$. Clearly the introduction of holes results in a notable improvement over the cell theory.[3] The range of agreement has been doubled, covering about the whole experimental region. No significant differences appear between the two assumptions and the curves obtained with different values of $s/3c$ are superimposable, within the scatter observed in the construction of the experimental universal curve. Results for $s/3c = 1.3$, corresponding to increased chain rigidity and not shown here, are in accord with this statement. An examination of eq 6 indicates that a change in $(s - 1)/s$ should have the same effect in the computation of y as a change in s/c.

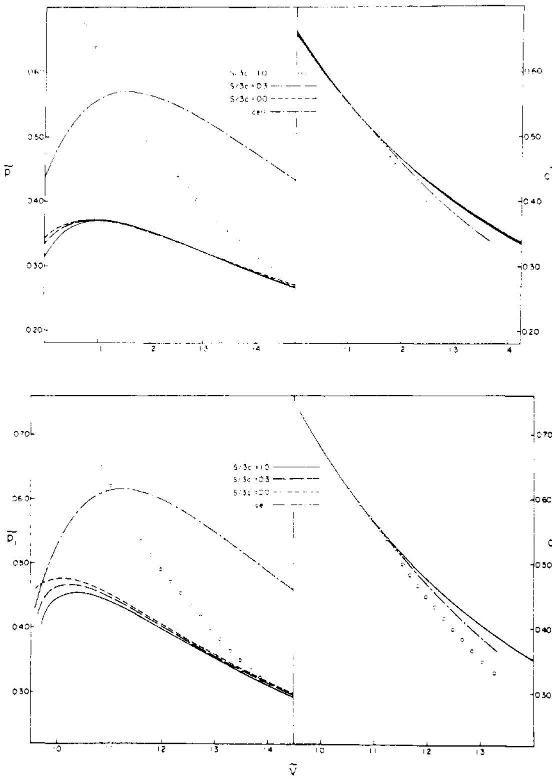

Figure 7. Reduced internal pressure and cohesive energy density as a function of reduced volume for polymer liquids, various values of s/c, and cell theory. Points, from experimental master curves. Top, assumption II, bottom, assumption I. Coordinate system as in Figure 5.

The results for $\tilde{p}_i$ and $\widetilde{\text{ced}}$ are presented in Figure 7 where the coordinate system corresponds to $s/3c = 1$. As previously,[3] the pressure shifting parameters were established by equating the theoretical and experimental values of the ced at a particular point, corresponding to $\tilde{V}(\text{cell}) = 1.16$ (in the cell coordinate system) and the values obtained are displayed in Table V. The final results are very similar for assumptions I and II. The curves for the cohesive energy density are superimposable but a slight separation for different s/c is noted in regard to the internal pressure. It should be noted that no adjustable parameter is left in the computation of $\tilde{p}_i$, and that with slightly different values for the reducing parameters, superposition could probably be achieved. The comparison with the cell theory[5] shows that for the $\widetilde{\text{ced}}$ the hole theory is successful in the same range as the former. The deviations are somewhat greater in the high-temperature region where, however, both theories are deficient. Furthermore, both the hole and the cell theory fail in describing the internal pressure function although now the maximum is displaced to the left, and the shape of the curve improved. This suggests that modifications in the hole theory may lead to better agreement in respect to $\tilde{p}_i$.

Finally the compressibility factor may be computed from eq 7, after solving the minimization condition at each volume and temperature. As can be predicted from the relation between the compressibility and the internal pressure, the use of assumptions I or II and of different values of s/c has the same effect as in $\tilde{p}_i$, that is, there is a slight difference between the results obtained with eq I-7 and II-7, and the curves corresponding to different values of s/c do not superimpose completely, when use is made of shifting parameters from the $\widetilde{\text{ced}}$. As an example we show in Figure 8 the compressibility

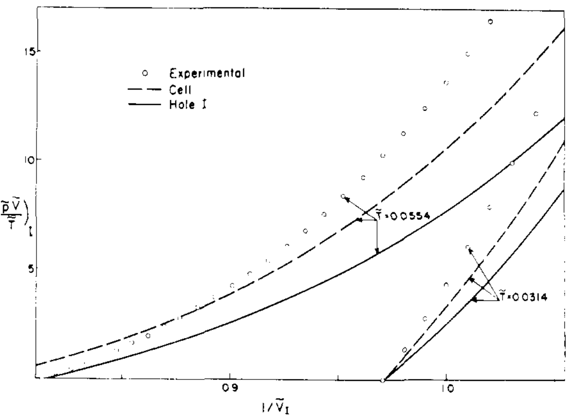

Figure 8. Reduced compressibility factor as a function of reduced density for polymer liquids at two reduced temperatures with assumption I and $s/3c = 1$.

factor computed at two reduced temperatures with assumption I and $s/3c = 1.0$. The experimental curves are plotted using the reduced Tait representation.[4] The theoretical curves are too flat which implies too high a compressibility. Since the expansivity at atmospheric pressure is correctly given, this result is consistent with the low values obtained for $\tilde{p}_i$, although the simple inverse relation between the internal pressure and the compressibility is valid at low pressure only. The cell theory curves are closer to the experimental results but at sufficiently high temperatures the inadequacy of this theory with respect to the $\tilde{V}$–$\tilde{T}$ function is again revealed.

The thermodynamic property for which most information is available in polymers is the atmospheric pressure isobar and here our theory is clearly successful. With respect to the energy and pressure properties the quantitative results are not superior to those of the cell theory. In any case the free volume theory offers the advantage of flexibility in formulation and thus the possibility of improved quantitative predictions.

V. Discussion

Any statistical mechanical treatment presupposes, of course, an explicit form of the intermolecular potential. We have followed the custom of adopting a 6–12 form and assuming pairwise additivity. In spherically symmetrical cases, deviations between theory and experiment have been ascribed to deficiencies in the statistical mechanical treatment. The inadequacies of the 6–12 potential at low densities have been repeatedly discussed, but it appears to represent a good effective pair potential for the dense fluid.[11]

Turning to inadequacies of the statistical mechanical model, we recall the square well approximation in the solidlike free volume, which may introduce errors because of the flat bottom and, at high temperatures, due to the repulsion. Moreover, specific assumptions had to be made in respect to the dependence of v_f on y. It has been pointed out by Blomgren[9] that a linear dependence of the free volume on y may be inadequate at low cell volumes. Finally, there is the uniformity in the hole size inherent in the lattice model.

In the case of chain liquids an additional assumption appears, that is the factorization of the cell partition function into c elements, see eq 1. Moreover, the use of a spherically symmetrical and pairwise additive potential at the close distances implied by the liquid state may be open to question for a structure such as a styrene segment or require a reformulation in terms of atom–atom interactions. One would like to gauge the influence of these simplifications by a comparison of the relation between theory and experiment for polymers, rare gases, and monomer-type molecules. However, different fitting procedures are involved, depending on the system. The mere fact that similar results are obtained for polymers with assumptions I and II, in contrast to the large difference observed in section III, emphasizes the necessity of treating the experimental data for chain liquids and argon in the same manner, if such a comparison is to be meaningful. This necessarily demands an identical superposition procedure of experimental and theoretical curves for argon and polymer systems.

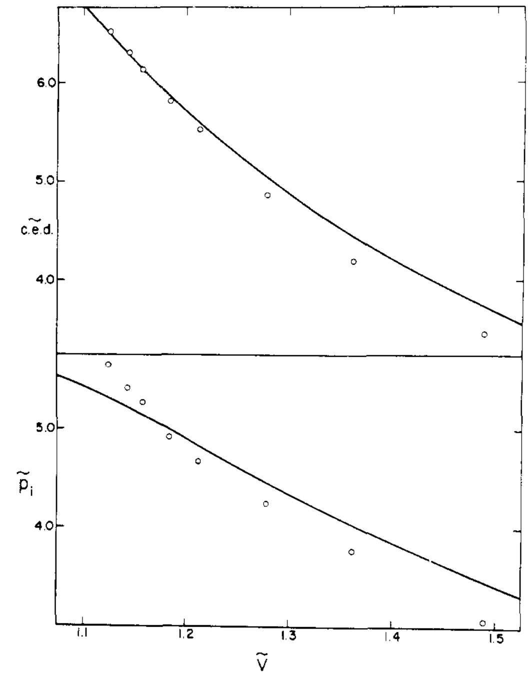

Figure 9. Reduced cohesive energy density and internal pressure as a function of reduced volume for liquid argon: curves, eq 8 and 9 with assumption I; points, experimental. For the reducing procedure see text, section V.

We start with the V–T data at low pressures, which can be fitted to the zero pressure function and yield $V^* = 25.06$ cm^3/mol and $T^* = 141.9$°K, compared with the 6–12 second virial coefficient values of 23.28 and 119.8. The pressure parameter is then derived by fitting the cohesive energy density at a particular point. We select $T = 90$°K and obtain $p^* = 319.12$ atm, compared with 412.54. The difference can arise from changes in ϵ^* and c (see below). Figure 9 shows the comparison between the theoretical c d's and $\tilde{p}_i$'s for spherical molecules and experimental values reduced with these new scale factors. With reduced volumes determined by a fitting of the V–T data, and reduced ced's derived from the initial region of the curve, the relative position of theory and experiment is similar in respect to the configurational energy to that seen in Figure 7 for polymers. The appearance of the $\tilde{p}_i$ curves is indeed different, but we recall that, whereas for nonpolar chain liquids p_i is generally about 10% larger than ced, for argon p_i turns out to be 10% smaller. Thus, if we can assume for small molecules experimental values of $\tilde{p}_i$ approximately 20% higher than in Figure 9, a behavior similar to the one for polymers, Figure 7 results. As for the compressibility factor, the relation between theory and experiment remains inverted for argon and polymer. We should mention here a difficulty already[5] encountered in this type of analysis, that is, the ratio p^*V^*/T^* for argon becomes different from unity. This could be ascribed to the existence of different effective values of ϵ^* when considering different properties, or to c being unequal to unity. In the first case we can define[5] factors f_T and f_p, and the principle of corresponding states remains valid if the ratio f_T/f_p is universal. In the case $p^*V^*/T^* = c$ and for argon we find $c = 0.69$. It is true that the theoretical curves used for the present comparison were computed with $s = c = 1$. However, whereas a change in these parameters leads to a new system of coordinates, the relative position of theoretical curves and experimental points is essentially unaffected by this change, as seen in Figures 6 and 7. In Figure 4, the lower temperature corresponds to the vapor region slightly above the critical point. However, the relation between theory and experiment is similar below T_c for reduced densities in excess of 0.55. That is, the computed compressibility factors (assumption I) are too large in the liquid region also. The revised reduction factors for argon shift the experimental points to the right on the abscissa and upward on the ordinate. The net result is a small displacement of the experimental curve to larger ordinate values. We conclude that an unequivocal difference between argon and polymer exists in respect to the computed compressibility coefficients, which are too large for the latter.

Argon is most appropriate as a testing ground for the various approximations current in liquid state theories. However, it may not represent the most suitable prototype of a monomer. The difference in the ratio ced/p_i between the two systems noted above once more underlines the need of repeating the analysis of section III and the comparison attempted in this discussion for other small molecules, such as benzene, carbon tetrachloride or representative monomers. The treatment of the ced data either masks or is insensitive to the expected differences in the potential function of argon and polymers. If further investigations show that monomer and polymer liquids differ only in respect to the compressibility factor, but not in the other properties investigated, it would suggest strongly that the factorization approximation in particular requires more detailed examination.

As first introduced,[1] a detailed evaluation of the chain dynamics in the environment of other chains has been replaced by the intuitive use of the dynamic parameter c, which is assumed to be independent of the variables of state. It is this assumption, of course, which has greatly facilitated the evaluation of the partition function. Using harmonic oscillator language, this requires strictly a separation of independent modes in the isolated chain into two groups of very high and very low frequencies relative to a characteristic lattice frequency with no intermediate region in the spectrum. In the real chain $3c$ can therefore only represent an apparent number of low-frequency modes. If this number is permitted to vary with V and T, a factorization of the total partition function into an external and internal part is no longer possible. Alternatively one may explicity include in the spectrum of the single chain a band of frequencies of magnitudes comparable with the lattice frequency. Such modifications would necessarily introduce characteristics of the particular polymer. Hence a principle of corresponding states would be invalidated, unless an argument is made that nonbonded interactions primarily determine the intramolecular rotational potentials and these can be related to the intermolecular potentials in the same manner for a series of related substances. This may be closer to reality in chains with bulky side groups than otherwise.

Acknowledgments. We wish to express our thanks to Mr. H. Roach of the Computer Sciences Laboratory, who has programmed the computations for this research. This work was partially supported by the National Aeronautics and Space Administration under Grant NsG-343 to the University of Southern California.